Size-dependent melting temperature of individual nanometer-sized metallic clusters

T. Castro and R. Reifenberger
Department of Physics, Purdue University, West Lafayette, Indiana 47907

E. Choi and R. P. Andres
School of Chemical Engineering, Purdue University, West Lafayette, Indiana 47907

(Received 20 April 1990)

Gold and silver clusters with diameters in the nanometer-size range were grown in an inert-gas beam and deposited on the end of a tungsten field emitter. The field-emission current from an individual cluster is used to study a size-dependent change in shape of the cluster as a function of temperature. Three experimental signatures indicate an abrupt change in cluster shape at a temperature below the bulk melting point. This temperature is found to depend on cluster size and is in agreement with a thermodynamic model for cluster melting, provided the cluster diameter is greater than ~ 2 nm.

I. INTRODUCTION

The details of how melting transition in a solid occurs has been a topic of long-term interest. Early theories of melting have focused on the role of vibrational instabilities,[1,2] lattice-shear instabilities,[3] catastrophic generation of dislocations,[4] or the presence of thermal vacancies or other point defects.[5] The dominant role played by an external surface in the melting transition has also recently been emphasized.[6] Clearly, interesting effects are expected in materials with large surface to volume ratios. Indeed, small Au clusters in the nanometer-size range exhibit a melting point depression.[7] From molecular-dynamic studies, there is considerable evidence that melting is initiated at external surfaces or along internal defects such as grain boundaries or dislocations. Computer calculations of melting have nicely simulated the influence of these features on the melting transition.[8,9]

The further study of melting in small nanometer-size clusters is relevant to a better understanding of the melting transition for a number of reasons. First, the melting of supported clusters possesses an inherent grain boundary at the cluster-substrate interface. Secondly, as cluster size decreases, the number of surface atoms increases and any role played by the surface in the melting transition will be accentuated. It is also well known that small clusters exhibit unique electronic and structural properties that often differ from their bulk solid-state counterparts.[10–13] These size effects have been investigated in both a theoretical and experimental way.[14–16] Also, the size-dependent melting of small clusters has received theoretical attention in the last few years.[17–22]

In spite of widespread interest in the melting transition of small clusters, there are still little data available on this interesting subject. All too often, the distribution in size of the clusters obscures the physics behind melting. Furthermore, most experimental techniques are incapable of resolving the melting temperature of an individual nanometer-size cluster. Those techniques, like transmission electron microscopy, capable of such resolution often produce surprising results, which are attributed to the inherently disruptive nature of the experimental technique. It therefore seems desirable to develop new approaches to further study the melting of small supported clusters.

In this paper we demonstrate the feasibility of using the field-emission current from an individual cluster to measure the melting temperature of that cluster. This new technique has the flexibility of studying a single isolated cluster whose diameter spans a wide range of sizes (~ 1–20 nm in diameter). Moreover, the experimental technique appears to be as sensitive to the large clusters as the small ones.

This paper begins with a description of a thermodynamic model of the melting of small particles. Although this simple model does not include the effects of the substrate on melting, we find it does predict the experimental results with reasonable accuracy for Au and Ag clusters with diameters greater than ~ 2 nm. The signatures for melting using the field-emission current technique are also discussed, followed by results for both gold and silver clusters. Data taken from the literature are compared with our results when possible. A summary is then given emphasizing the important aspects of the work.

II. THEORETICAL CONSIDERATIONS

In principle, any theoretical description of a melting transition should strive to answer questions concerning the structural rearrangement of atoms that occurs during the melting process. In practice, an alternative approach is often taken using classical thermodynamics to describe cluster melting. The thermodynamic approach does not require information about the position of the atoms comprising the cluster. All that is necessary is a thermodynamic condition describing phase coexistence between the solid and liquid cluster along with some general thermodynamic relationships. Phenomenological models of

this type have been reviewed in the literature.[23–25] We will briefly describe the model presented by Buffat and Borel.[7] In this model the cluster is assumed to have a spherical shape both before and after melting takes place. In addition, substrate-cluster interactions are not accounted for.

Within the framework of this model the basis for a depression in the melting point of small clusters is a direct consequence of the large internal stress acting on a cluster due to the presence of its surface. The differential pressure drop across the surface of a spherical cluster (solid or liquid) of radius r_c, and having a surface tension γ may be shown to be[26]

$$P - P_{\text{ext}} = 2\gamma / r_c \ . \tag{1}$$

Since our experiments are carried out in a ultra-high vacuum (UHV) environment, there is negligible external pressure, P_{ext}, applied to the cluster. Equation (1) suggests that a 3-nm diameter gold cluster ($\gamma \sim 1.3$ J/m^2) is under the influence of an internal pressure of ~ 8500 torr (~ 11 atmospheres).

The condition for phase coexistence may be expressed by setting the chemical potentials of the liquid and solid phase equal.[27,28] The chemical potential for a cluster is modified (compared to the bulk value) due to the presence of the pressure term given in Eq. (1). By expanding the chemical potential, $\mu(T,P)$ at a specific temperature and pressure about the corresponding bulk value $\mu_0(T_0,P_0)$, one obtains to first order

$$\mu(T,P) = \mu_0(T_0,P_0) + \frac{\partial \mu}{\partial T}(T - T_0) + \frac{\partial \mu}{\partial P}(P - P_0) \ , \tag{2}$$

where T_0 and P_0 are the values of the melting temperature and the equilibrium vapor pressure at the bulk triple point. Since Au and Ag have low vapor pressures at the triple point, T_0 may safely be taken as the bulk melting temperature of the material.[2]

The use of the Gibbs-Duhem relationship[28,7] permits an evaluation of the partial derivatives through

$$S dT - V dP + M_c d\mu = 0 \ ,$$

where, S is the entropy of the cluster, V is the cluster volume and M_c is the cluster mass. From this equation the following two thermodynamic identities result:

$$\frac{\partial \mu}{\partial T} = \frac{-S}{M_c} \equiv s \ ,$$

$$\frac{\partial \mu}{\partial P} = \frac{1}{\rho} \ .$$

In these two equations ρ is the mass density of the cluster and s is the entropy per unit mass. Inserting these two equations into Eq. (2), and using the condition that the chemical potentials are equal in both the solid and liquid phases at the melting point, one finds the following expression at equilibrium:

$$(s_s - s_l)(T_m - T_0) - P_l/\rho_l + P_s/\rho_s - P_0(1/\rho_s - 1/\rho_l) = 0 \ , \tag{3}$$

where the subscripts s and l represent the solid and liquid phases of the cluster at the melting point T_m.

In this model it is assumed that the clusters are spherical during the melting process. Conservation of the number of atoms, before and after melting gives $r_{cs}^3 \rho_s = r_{cl}^3 \rho_l$, where r_{cs} and r_{cl} are the radii of the solid and liquid cluster, respectively. It is also easy to show that the term containing P_0 is small compared to the other quantities and is therefore neglected. Using this result along with Eq. (1), Eq. (3) may be expressed as

$$(1 - T_m/T_0) = \frac{2}{\rho_s L r_c}[\gamma_s - \gamma_l(\rho_s/\rho_l)^{2/3}] \ . \tag{4}$$

In this equation, $r_c \equiv r_{cs}$ for the sake of brevity, $L \equiv (s_l - s_s)T_0$, is the latent heat of fusion of the bulk phase, $\gamma_s(\gamma_l)$ are the surface tensions of the solid (liquid) bulk material near the melting point. Equation (4) was first derived by Pawlow[29] and then reevaluated by Hanszen.[30] This equation predicts that a plot of the inverse cluster radius versus T_m/T_0 will yield a straight line.

If the depression of the melting temperature predicted by Eq. (4) is large, then the change in the appropriate thermodynamic variables with temperature must be taken into account. This can be done by expanding $\gamma/(\rho r)$ as follows:

$$\left.\frac{\gamma}{\rho r}\right|_T = \left.\frac{\gamma}{\rho r}\right|_{T_0} + \frac{\partial}{\partial T}\left(\frac{\gamma}{\rho r}\right)_{T_0}(T - T_0) + \cdots \ . \tag{5}$$

Defining α, the linear expansion coefficient, as $\alpha \equiv -(1/r)\partial r/\partial T$ and $\eta \equiv -(1/\gamma)\partial\gamma/\partial T$, Eq. (5) evaluated at the melting temperature of the clusters becomes

$$\left.\frac{\gamma}{\rho r}\right|_{T_m} = \left.\frac{\gamma}{\rho r}\right|_{T_0} - \left.\frac{\gamma(\eta - 2\alpha)}{\rho r}\right|_{T_0}(T_m - T_0) + \cdots \ , \tag{6}$$

where all the parameters in the above equation apply to the cluster in either the liquid and solid phases. Equation (6) may be combined with Eqs. (1) and (3) to obtain the following correction to the Pawlow theory:

$$(1 - T_m/T_0) - \frac{2}{L\rho_s r_c}[\gamma_s - \gamma_l(\rho_s/\rho_l)^{2/3}] - \frac{2T_0}{\rho_s L r_c}[\gamma_s(\eta_s - 2\alpha_s) - \gamma_l(\eta_l - 2\alpha_l)(\rho_s/\rho_l)^{2/3}](1 - T_m/T_0) = 0 \ . \tag{7}$$

The third term in Eq. (7) partially corrects the assumption that the surface tension of a cluster can be well approximated by the surface tension of a bulk solid. Since surface tension changes with temperature,[31] decreasing as the temperature is increased, larger values of γ should be used. This is the origin of η in the above expression. 2α is a measure of the increase in surface area that occurs upon heating. Since the surface tension is the surface free

TABLE I. The values of the thermodynamic quantities of bulk gold needed in order to apply Eq. (7) to the experimental results. The references that were used to obtain these values are also given. The table is an updated adaptation of the one presented in Ref. 7.

		Solid		Liquid	
Name	Symbol	Value	Reference	Value	Reference
Mass density	$\rho(\mathrm{kg/m^3})$	1.84×10^4	Ref. 46, pp. 4–124 Ref. 23	1.728×10^4	Ref. 47, p. B-221 Ref. 23
Surface Tension	$\gamma(\mathrm{J/m^2})$	1.29–1.42	Ref. 23 Ref. 31, p. 124	1.135	Ref. 23 Ref. 31, p. 102 Ref. 32, p. 403
	$\partial\gamma/\partial T(\mathrm{J/m^2K})$	-4.33×10^{-4}	Ref. 31, p. 124	-1.0×10^{-4}	Ref. 32, p. 403
Linear Expansion Coefficient	$\alpha(\mathrm{K^{-1}})$	2.31×10^{-5}	Ref. 46, p. 4–124	2.10×10^{-5}	Ref. 47, p. B-221
Latent Heat	L(J/kg)	6.276×10^4	Ref. 47, p. D-187		
Melting Temperature	T_0(K)	1336	Ref. 33, p. 50		

energy per unit surface area,[31] this term corrects for the decrease in surface tension that occurs for a given temperature rise. If $\eta=2\alpha$, the correction term is zero and the Pawlow theory prevails. The numerical values used to evaluate the coefficients in this equation for T_m/T_0 are discussed in the Appendix.

In applying this model to the experimental results, γ_s is the only free parameter that we have chosen to vary. This choice is partly due to the sensitivity of Eq. (7) to variations in the surface tension. There appears to be good agreement between different authors for γ_l. However, results for the solid surface tension vary as shown in Tables I and II.

Field emission from a cluster. In a previous article[34] it was shown that the field-emission current density, J, from a supported gold cluster obeys the well-known Fowler-Nordheim law for field emission[35]

$$J = AF^2\exp\left[\frac{-b\phi_c^{3/2}v(y)}{F}\right], \tag{8}$$

where b is a known constant, ϕ_c is the cluster work function, F is the average field over the cluster surface and $v(y)$ is a slowly varying function of $y=e^3F/\phi^{1/2}$. F is related to the voltage, V, applied to the tungsten tip by

$$F=K\beta V\ . \tag{9}$$

In this expression β is a geometrical factor relating the applied voltage to the electric field far from the cluster, and K is the field enhancement factor which depends solely on the geometry of the cluster relative to the substrate. Combining the above two equations J may be written as

$$J = AF^2\exp\left[\frac{-b\phi_c^{3/2}v(y)}{K\beta V}\right]. \tag{10}$$

A plot of the $\ln(J/V^2)$ over $1/V$ will yield a straight line with slope, S given by

$$S=-\frac{b\phi_c^{3/2}s(y)}{K\beta}\ . \tag{11}$$

The physical basis for measuring the melting temperature of a single supported cluster relies on the sensitivity of Eq. (10) and Eq. (11) to changes in K. In principle, for a given cluster shape, K may be calculated as was de-

TABLE II. Numerical values for the thermodynamic quantities of bulk silver need to evaluate Eq. (7). The references which were used to obtain these values are also given.

		Solid		Liquid	
Name	Symbol	Value	Reference	Value	Reference
Mass density	$\rho(\mathrm{kg/m^3})$	9.82×10^3	Ref. 46, pp. 4–130	9.33×10^3	Ref. 47, p. B-221
Surface Tension	$\gamma(\mathrm{J/m^2})$	1.1–1.2	Ref. 44 Ref. 45	0.895	Ref. 31, p. 102 Ref. 32, p. 403
	$\partial\gamma/\partial T(\mathrm{J/m^2K})$	-4.70×10^{-4}	Ref. 31, p. 125	-1.3×10^{-4}	Ref. 32, p. 403
Linear Expansion Coefficient	$\alpha(\mathrm{K^{-1}})$	3.03×10^{-5}	Ref. 46, pp. 4–130	3.29×10^{-5}	Ref. 47, p. B-221
Latent Heat	L(J/kg)	1.11×10^5	Ref. 47, p. D-187		
Melting Temperature	T_0(K)	1234	Ref. 33, p. 20		

scribed in a previous paper.[36] An important consequence of Eq. (10) is that for a given applied voltage V, the field-emission current from a cluster is greatly enhanced relative to the substrate. The high sensitivity of current to overall cluster geometry allows one to measure the temperature at which the cluster shape changes. The shape change is interpreted as a solid-liquid transition which enables the cluster to spread out and wet the surface.

In our field-emission experiment, there are three signatures that indicate when a cluster has undergone such a transition. The first is a change in the overall field-emission pattern from the cluster. The field-emission spot size on the fluorescent screen, created by electron emission from an isolated cluster, depends on the geometry of the cluster on the support. A change in shape of the supported cluster will result in a change in spot size on the fluorescent screen. Whether the spot size increases or decreases depends on the detailed morphology of the cluster surface after wetting occurs. In a field-emission experiment it is difficult to determine this morphology from an image. The important fact is that changes in shape can be detected.

The second signature is the change in voltage required to draw a constant current from the cluster. The current is exponentially dependent on the field enhancement factor. When the cluster melts and wets the surface the field enhancement factor K decreases. This causes the voltage required to draw the same current from the cluster to increase. This increase is typically ~ 200 V, a voltage increment which is easily measured.

The third signature for cluster melting is a change in the Fowler-Nordheim slope [Eq. (11)] upon heating. For a fixed work function, large changes in slope may be interpreted as corresponding changes in cluster shape. It is found experimentally that the slope increases after heating. This implies a decrease in K which is consistent with the interpretation that the cluster spreads over the surface.

A more complete discussion of these three signatures can be found elsewhere.[37] In presenting the experimental results in the next section, the three criterion for melting have been used to extract the melting temperature of a single supported cluster.

III. RESULTS

A. Experimental details

The experimental setup and procedures used to deposit a single performed cluster on a field emitter have been described in detail elsewhere.[36,37] Briefly, the system is composed of a multiple-expansion cluster source[38,39] and a stainless steel, ultra-high-vacuum chamber suitable for field-emission experiments. Clusters of controlled mean size are grown in an inert-gas beam. A field emitter is briefly exposed to the beam and then transferred to a field-emission chamber in a vacuum transfer cell at pressures of $\sim 5\times 10^{-8}$ torr. Experiments are performed in the field-emission chamber operating at a pressure of $\sim 2\times 10^{-10}$ torr. The field-emission apparatus is equipped with a digital image acquisition system which allows a detailed analysis of cluster images to be performed.

In measuring size dependent properties an adequate method for size determination must be used. Due to the difficulties in measuring the size accurately from the field-emission image, independent methods were employed in this work.[37,38] In general, cluster diameters were determined by transmission electron microscopy (TEM) analysis described elsewhere.[36,37] In the data presented below, cluster diameters and their experimental uncertainties are taken to be the mean and one standard deviation determined from the TEM analysis.

The experiments are performed in the following way. After a single cluster is placed on the end of a field emitter, the sample is inserted into the field-emission chamber and a Fowler-Nordheim plot is taken. This requires 6 to 9 measurements of the field-emission current as a function of the applied voltage. This data is then plotted in order to determine the slope as given by Eq. (10). Typically, a digital image of the field-emission pattern of the cluster is recorded with the image acquisition system at the mean voltage used when measuring the Fowler-Nordheim slope. The tip is then heated in *zero electric field* to a given temperature for $\sim 10-30$ sec. Temperature measurements are made with a thermocouple spot welded to a tungsten loop supporting the tip.[36] After the tip cools to room temperature, another Fowler-Nordheim plot is taken along with a digital image of the field-emission pattern. Typical heating steps range from 10 to 40 K. The entire procedure is repeated until a temperature is reached which causes the cluster shape to suddenly change.

In Fig. 1(a), a three-dimensional representation of the field-emission current from a ~ 20-nm diameter gold cluster taken after heating the tip (i.e., substrate) to 1327 K. The x-y coordinates in this plot are proportional to the position of the image on a nearby fluorescent screen. The z coordinate represents the light intensity distribution on the fluorescent screen which is directly proportional to the field-emission current density.[37] Figure 1(b) shows an image of the same cluster after heating to 1330 K. Notice the increase in size of the image as compared to that in Fig. 1(a). This increase also correlates with an increase in the applied voltage required to draw the same field-emission current. In addition to these two signatures, a sharp change in the Fowler-Nordheim slope is also observed at 1330 K. This is shown in the lower portion of Fig. 2. This temperature is close to the bulk melting temperature of gold (1336 K). The above three observations are in agreement with the scenario for cluster melting; as the cluster melts and wets the surface, the field enhancement factor K decreases. Due to this decrease, (i) the current at a specified voltage drops [Eq. (10)], (ii) the Fowler-Nordheim slope will increase [Eq. (11)] and (iii) the size of the image on the fluorescent screen changes.

Figure 2 also shows a plot of the Fowler-Nordheim slope as a function of temperature for $a \sim 1.5$-nm diameter gold cluster. In this case the Fowler-Nordheim slope changes at a lower temperature than that for the 20 nm cluster. In addition, the variation in slope occurs over a

broader temperature range than observed for the 20 nm cluster. It is interesting to speculate on this observation. Challa[19] has demonstrated through computer simulation that temperature driven transitions become smeared out for finite systems compared to their bulk solid-state counterparts. This is in agreement with other theoretical models on cluster melting reported in the literature.[17,21] However, it is too early to tell if this is experimentally the case.

B. Size-dependent melting of Au clusters

Similar experiments were performed on different clusters, using the three signatures for cluster melting, in order to determine their melting temperature as a function of size. A melting temperature range may then be as assigned to each cluster diameter studied. The results for gold clusters melting on tungsten are presented in Fig. 3. Our experimental points are given by solid dots. The data marked by x's are take from Fig. 5 of Ref. 7, and Fig. 5(b) of Ref. 23. In Ref. 23, data was collected for gold particles >10 nm. Since our interest in this study is really clusters with diameters less than this, these points

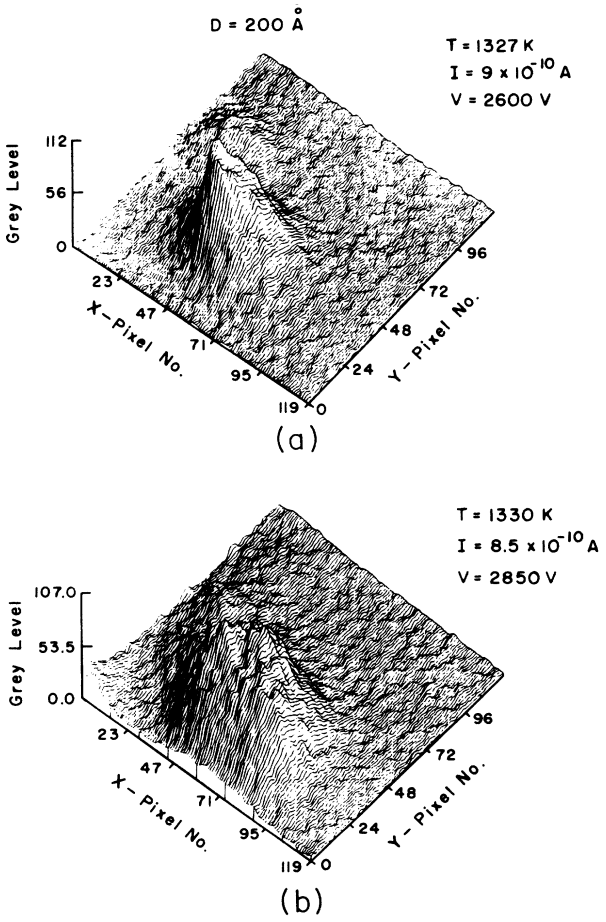

FIG. 1. A digitized, three-dimensional field-emission pattern of a 20-nm diameter gold cluster (a) taken *after* heating to 1327 K and (b) *after* heating to 1330 K. The voltage necessary in order to draw approximately the same field-emission current is also listed.

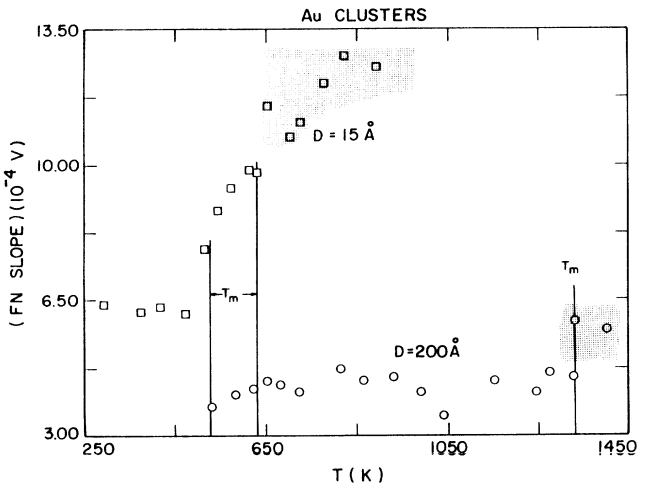

FIG. 2. A plot of the Fowler-Nordheim slope as a function of temperature for a 1.5 nm diameter and a 20-nm diameter Au cluster. The shading on each curve indicates where substrate emission is contributing to the current measurement. Substrate emission will become significant only after the cluster has melted. Before melting, the high radius of curvature of the cluster with respect to the substrate ensures that only electron emission from the cluster is observed. The vertical lines marking the 1.5 nm curve provide an estimate for the uncertainty in the melting temperature. The vertical line marking the melting temperature for the 20 nm cluster agrees well with the bulk melting temperature of Au.

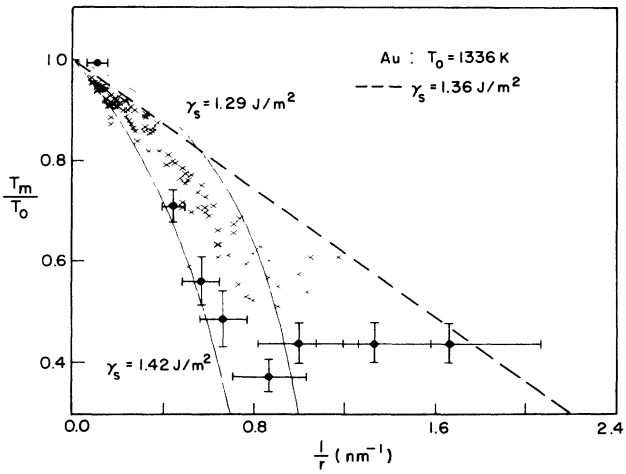

FIG. 3. A plot of the relative lowering of the melting point for gold clusters vs the inverse cluster radius. The solid circles represent the values determined from this work. The x's are data points taken from Refs. 7 and 23. The thermodynamic model [Eq. (7)] is given by the solid lines for two different values of solid surface tension as indicated. The dash line is that predicted by the Pawlow theory for a mean solid surface tension of 1.36 J/m^2.

will not be discussed further. In general, the uncertainty in temperature for our data are due to the uncertainties in identifying the transition from the Fowler-Nordheim slopes. It should be noted that the 1.5-nm and 3.0-nm-diameter samples were reproduced, yielding melting temperatures within the error shown.

The thermodynamic prediction, according to Eq. (7) is given by the solid lines (see Table I). The calculations reveal that the thermodynamic model is sensitive to the value of the solid surface tension. Notice that both curves bracket our data as well as the data taken from Ref. 7 up to a cluster diameter of ~ 2.0 nm. Below this size there is a definite deviation from the model. Also shown in this figure is the prediction of the Pawlow theory [Eq. (4)]. This is given by the dashed line which was calculated using a surface tension of 1.36 J/m^2. This figure shows that the correction terms included in Eq. (7) are necessary in order to explain the experimental results.

The data from this study systematically lie below the data taken from Ref. 7 which measured the integrated diffraction intensities from an ensemble of different size gold clusters supported on an amorphous carbon substrate as a function of temperature. The melting temperature extracted from a diffraction experiment depends on the Debye-Waller factor for the clusters. If this value is treated as an adjustable parameter, a lower melting temperatures for the smaller clusters will result.[7] This analysis will force the x's to move closer to our experimental data for diameters less than ~ 5 nm.

Taking into account the difference in the experimental techniques, it is surprising that the agreement is this good. Our measurements involve studying single isolated gold clusters supported on W substrates. Reference 7 investigates an ensemble of clusters taking into account their size distribution. This explains the spread in the x data points, especially at small sizes. The interaction between gold and tungsten is relatively strong[40] being ~ 3 eV/atom. That between carbon and gold is considerably weaker. During our experiments the clusters wet the substrate. The particles in Ref. 7 do not. The difference between our data and those reported in Ref. 7 may well be due to the difference in interaction energy for Au on W and Au on C.

Another interesting feature about Fig. 3 is the saturation region that occurs for diameters less than 2 nm. Although the thermodynamic model probably breaks down below this diameter, substrate effects cannot be ruled out. Since the substrate interaction is strong, one might expect a saturation in the melting temperature for the smaller diameter clusters.

C. Size-dependent melting of Ag clusters

The procedure used to measure the melting temperature of supported silver clusters is identical to the technique discussed above for gold. A unique feature of the Ag cluster study is the reproducible torus-shaped field-emission pattern for all Ag clusters investigated [see Fig. 4(a)]. This pattern was always observed after insertion into our field-emission chamber and disappeared after heating the Ag cluster to ~ 400 K as shown in Fig. 4(b). This torus-shaped geometry is apparently related to faceting of the Ag cluster. It is well-known from field-emission studies that for a fixed applied voltage, flat facets produce a smaller field-emission current than the surrounding facet edges due to electric-field enhancements on the edges with respect to the facet. Whether the faceting is an inherent structural property of the clusters used in this study[41] or is due to the background gas present during sample transfer ($< 1 \times 10^{-7}$ Torr) cannot be decided at this time.

All data points for the Ag clusters were plotted with TEM size confirmation. As in the case for Au, a plot of the Fowler-Nordheim slope versus temperature shows an abrupt change in slope. Typically, the slope changes by a factor of ~ 3. This increase in slope roughly coincides with a change in the field emission pattern. However, in the case of Ag, a *decrease* in the size of the field-emission pattern from an individual cluster was found. This characteristic was continually observed throughout this study for Ag clusters and should not necessarily be interpreted as an indication of a smaller cluster on the W support after melting. A change in cluster morphology may

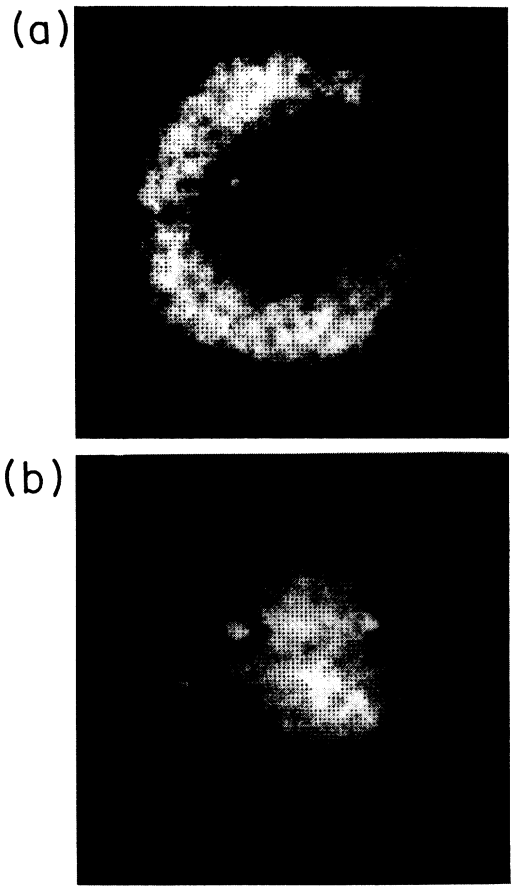

FIG. 4. A digital field-emission pattern of ~ 80 Å diameter Ag cluster taken after placing the sample into the field-emission chamber. In (a), the pronounced torus-shape geometry is clearly evident. The same sample after heating the substrate to ~ 400 K is shown in (b). The torus-shape configuration has vanished.

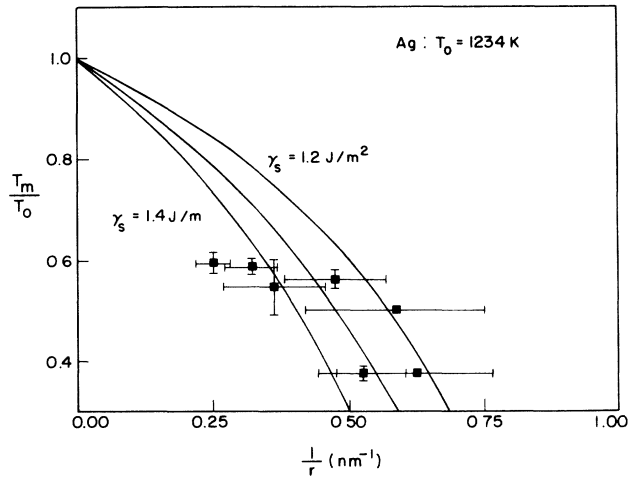

FIG. 5. A plot of the relative lowering of the melting point for silver clusters as a function of inverse cluster radius. Three different curves, predicted by Eq. (5) for three different solid surface tensions of 1.2, 1.3, and 1.4 J/m^2 respectively, are given by the solid lines.

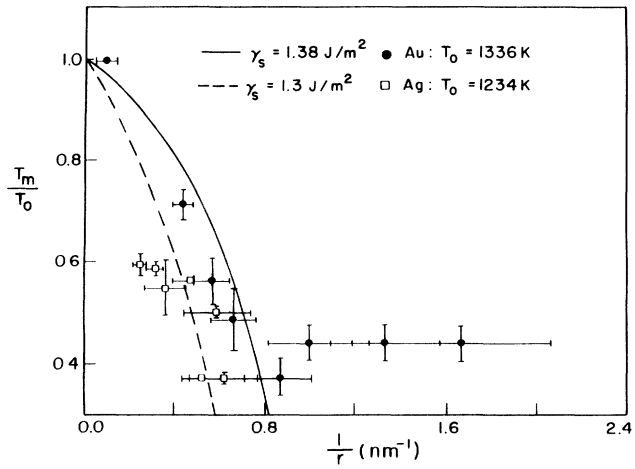

FIG. 6. A plot of the melting point depression for silver and gold clusters studied in this work as a function of inverse cluster radius. Reasonable fits to the data according to the thermodynamic model [Eq. (5)] are shown by the two solid curves for solid surface tensions of, 1.38 J/m^2 for gold, and 1.30 J/m^2 for silver.

decrease the magnification of the field-emission image in such a way to produce this effect[37] even though the cluster has wet the surface. For all the silver clusters studied, an increase in voltage was always required in order to draw constant current from a cluster after cluster melting had occurred.

A compilation of the silver cluster data taken are presented in Fig. 5. Also shown in this figure are three curves computed using the thermodynamic model Eq. (7) with three different solid surface tensions, of 1.2, 1.3, and 1.4 J/m^2, respectively. The curves again reveal the sensitivity of the model to slight surface tension variations. In general, the model predicts the overall trend in the data. From the data it is clear that a solid surface tension of $\gamma_s \sim 1.3$ J/m^2 provides the best fit. This is ~ 0.1 J/m^2 larger then the values obtained for silver by others (1.1–1.2 J/m^2) as listed in Table II.

IV. SUMMARY

Figure 6 summarizes the important aspects of this work by comparing the gold and silver data taken with the field-emission technique. When the data are displayed in this way a clear distinction between gold and silver clusters is apparent. For a fixed diameter, silver clusters melt at a lower temperature than gold. This is in agreement with the thermodynamic model for cluster melting [Eq. (7)]. This is indicated in the figure by the two solid lines which represent reasonable fits to the data. These curves are drawn with solid surface tensions of, $\gamma_s = 1.38$ J/m^2 for gold, and $\gamma_s = 1.30$ J/m^2 for silver. The best value of γ_s for gold is in excellent agreement with those obtained by others.[23,7] However, the value of γ_s deduced for silver is low by ~ 0.1–0.2 J/m^2 compared to values listed in the literature. This may be due to the unavoidable contamination of the silver clusters that occurs during sample transfer. It is well known that silver oxidizes fairly rapidly while gold does not.[42] It is also true that surface tension depends on crystal purity.[31] These facts, taken together, may explain the deviation observed here.

An important result from the gold study is the saturation of the melting temperature observed for clusters with diameters less than ~ 2 nm. We do not expect the thermodynamic model to accurately describe the melting of very small clusters and other substrate-cluster systems need to be investigated in order confirm such a conclusion. This was the motivation for studying silver clusters on tungsten. The interaction between silver and tungsten is weaker than that between gold and tungsten[43] as indicated by thermal desorption spectroscopy data. These results show a range in binding energies of 2.8–3.55 eV/atom for Ag on W(110) and 3.3–4.1 eV/atom for Au. Thus, the thermodynamic model may fit the silver data better at lower sizes than gold. Unfortunately, smaller Ag clusters could not be obtained. Future studies on both strong and weakly interacting substrates using the field-emission technique should be performed.

Finally, a number of alternative explanations for the data should be discussed. Basically, the change in field-emission current measured in this study can be produced by either electronic or structural changes to the cluster. In particular, either the work function ϕ or the field enhancement factor K appearing in Eq. (9) can change.

As discussed in a previous paper,[34] changes in work function alone can be ruled out. Sudden work function changes between 2.5 and 5 eV are required to explain the change in the Fowler-Nordheim slope found in this study. The size of this change is too large to be taken as a likely explanation of the data.

Changes in the cluster field enhancement facator K due to structural mechanisms other than melting can also be

considered and discounted in turn. For instance, the cluster could rearrange on the tip at a particular temperature, resulting in a change of the field-emission current due to its change in position. Examination of the image of the clusters showed no relative motion of the cluster over the substrate. The high magnification of the field-emission geometry would easily reveal such motion and any explanation of our data based on only a change in position of the cluster is not viable.

Accelerated evaporation of the clusters as the temperature is increased might be invoked to explain the observed change in K. The evaporation of small Au and Ag particles has been studied by Sambles *et al.*[23,44,45] and an experimental verification of the Kelvin equation resulted. Relying on their experiments, it is possible to estimate the time rate of change of the cluster diameter as a function of temperature. Calculations show that the time required to evaporate clusters in our size range are two to four orders of magnitude longer than the maximum heating time employed in our experiments. For this reason, evaporation can be dismissed as a possible mechanism for a change in the geometrical factor K.

Another possibility is to attribute a change in cluster shape to Young's equation which is often used to predict the equilibrium geometry of two different materials in contact with each other. Since the surface tensions of the cluster and substrate are known to be weakly dependent on temperature, it might be possible for the contact angle between cluster and substrate to vary with temperature. It might be argued that this mechanism produces a change in shape of the cluster that accounts for our experimental observations. Apart from predicting a reversible transition, a result in conflict with the data, the magnitude of the change in contact angle can be estimated and found to be too small to account for our observations.

It might also be argued that a thermally activated diffusion of the atoms comprising a cluster might explain our data. The rate of diffusion is strongly influenced by the activation energy which in turn depends on the details of the microscopic substrate geometry as well as adsorbates. *A priori,* it is difficult to rule out all possible scenarios of changes in cluster shape based on thermally activated diffusion alone. However, a number of experiments were performed in which the cluster was heated to the same temperature (below the cluster melting point) for different periods of time and the resulting field-emission images were examined for detectable changes. For example, a 2 nm Au cluster showed no significant change in shape (i.e., in the Fowler-Nordheim slope) after repeated heating to 425 and 490 K for heating times ranging between 15 and 20 secs. A similar experiment on a 5.5-nm diameter Ag cluster heated to 440 K also showed no significant change in cluster shape. These observations seem to rule out an explanation based on surface diffusion to explain our data. Furthermore, for diffusion to explain our data, an abrupt change in the diffusion rate of the atoms comprising the cluster across the tungsten surface must occur at a temperature which depends inversely on the cluster radius. Such a size-dependent diffusion mechanism seems unlikely and is also tentatively ruled out as a possible explanation of our results.

We conclude that the data presented do in fact measure the size dependent melting of Au and Ag clusters. Quantities of traditional interest like the order of the melting transition or the variation of the order parameter near the transition are not easily measured by our field-emission technique. Other quantities like the influence of the substrate on the melting transition and the nature of the melting transition for bimetallic clusters comprised of two different metals are topics that can be readily addressed using the versatile cluster source and the field-emission technique described above.

ACKNOWLEDGMENTS

This work was partially supported by U.S. Department of Energy (DOE) Contract No. DE-FG-02-88ER451162. T. Castro would also like to thank the David Ross Foundation at Purdue University for financial support during the latter stages of this work. The authors acknowledge helpful discussions with S. B. Park, Y. Z. Li, and Mongea Lin throughout this work.

APPENDIX

Accurate values for the thermodynamics variables appearing in Eq. (7) are required. The values used in Eq. (7) are given in Table I for gold and in Table II for silver.

All the parameters should be evaluated for the solid or liquid phases of the bulk substances at the melting point. Some of these values could not be found in the literature for the temperatures of interest. This is true for the linear expansion coefficient and the bulk solid-state mass density, ρ_s. To remedy this situation, α_s was determined by fitting the available temperature dependent data[46] to a third-order polynomial and then extrapolating to T_0. Once the coefficients in the fitting polynomial were determined, ρ_s was computed by using the definition of α and the well-known mass density at room temperature of the elements.[44] This approach yields a value of $\rho_s(T_0)$ for gold that is in excellent agreement with the value used by others.[23] The mass density of the elements in the liquid state at the melting point and above are fairly well known.[47] A polynomial fit to this data allows a value for α_l to be obtained through the relationship $\alpha \equiv (\frac{1}{3}\rho) d\rho/dT$ where ρ is the density.

[1]F. A. Lindemann, Z. Phys. **11**, 609 (1910).
[2]A. R. Ubbelohde, *The Molten State of Matter* (Wiley, New York, 1978).
[3]L. L. Boyer, Phase Transitions **5**, 1 (1985).
[4]R. M. J. Cotterill, J. Cryst. Growth **48**, 582 (1980).
[5]R. W. Cahn, Nature **273**, 491 (1978).
[6]R. W. Cahn, Nature **323**, 668 (1986).
[7]Ph. Buffat and J. P. Borel, Phys. Rev. A **13**, 2287 (1976).
[8]J. F. Lutsko, D. Wolf, S. R. Phillpot, and S. Yip, Phys. Rev. B **40**, 2841 (1989).

[9]S. R. Phillpot, J. F. Lutsko, D. Wolf, and S. Yip, Phys. Rev. B **40**, 2831 (1989).
[10]J. B. Barner and S. T. Ruggiero, Phys. Rev. Lett. **59**, 807 (1987).
[11]James R. Chelikowsky, Phys. Rev. Lett. **60**, 2669 (1989).
[12]Sumio Iijima and Toshinari Ichihashi, Jpn. J. Appl. Phys. **24**, L125 (1985).
[13]J. Farges *et al.*, in *Physics and Chemistry of Small Clusters,* edited by P. Jena, B. K. Rao, and S. N. Khanna (Plenum, New York, 1987), p. 15.
[14]L. Genzel, T. P. Martin, and U. Kreibig, Physik B **21**, 339 (1975).
[15]S. H. Suck Salk and C. K. Lutrus, J. Chem. Phys. **87**, 636 (1987).
[16]A. vom Felde, J. Fink, and W. Ekardt, Phys. Rev. Lett. **61**, 2249 (1988).
[17]J. Ross and R. P. Andres, Surf. Sci. **106**, 11 (1981).
[18]R. Stephen Berry, Julius Jellinek, and Grigory Natanson, Phys. Rev. A **30**, 919 (1984).
[19]Murty S. S. Challa and D. P. Landau, Phys. Rev. B **34**, 1841 (1986).
[20]Estela and Blaisten-Barojas, I. L. Garzon, and M. Avalos, Phys. Rev. B **36**, 8447 (1987).
[21]Thomas L. Beck, Julius Jellinek, and R. Stephen Berry, J. Chem. Phys. **87**, 545 (1987).
[22]R. Stephen Berry and David J. Wales, Phys. Rev. Lett. **63**, 1156 (1989).
[23]J. R. Sambles, Proc. R. Soc. London A **324**, 339 (1971).
[24]S. J. Peppiatt and J. R. Sambles, Proc. R. Soc. London A **345**, 387 (1975).
[25]C. J. Coombes, J. Phys. F **2**, 441 (1972).
[26]I. Prigogine, R. Defay, and A. Bellemans, *Surface Tension and Adsorption* (Wiley, New York, 1966).
[27]Charles Kittel and Herbert Kroemer, *Thermal Physics* (Freeman, San Francisco, 1980).
[28]F. Reif, *Fundamentals of Statistical and Thermal Physics* (McGraw-Hill, New York, 1965).
[29]P. Pawlow, Z. Phys. Chem. **65**, 1 (1909).
[30]K. J. Hanszen, Z. Phys. **157**, 523 (1960).
[31]Lawrence E. Murr, *Interfacial Phenomena in Metals and Alloys* (Addison-Wesley, Reading, 1975).
[32]V. K. Semenchenko, *Surface Phenomena in Metals and Alloys* (Pergamon, New York, 1961).
[33]Ralph Hultgren *et al.*, *Selected Values of the Thermodynamic Properties of the Elements* (American Society for Metals, Metals Park, Ohio, 1973).
[34]T. Castro, Y. Z. Li, R. Reifenberger, E. Choi, S. B. Park, and R. P. Andres, J. Vac. Sci. Technol. A **7**, 2845 (1989).
[35]A. Modinos, *Field, Thermionic and Secondary Electron Emission Spectroscopy* (Plenum, New York, 1984).
[36]T. Castro, R. Reifenberger, E. Choi, and R. P. Andres, Surf. Sci. (to be published).
[37]T. Castro, Ph.D. thesis, Purdue University, 1989 (unpublished).
[38]Seung Bin Park, Ph.D. thesis, Purdue University, 1988 (unpublished).
[39]E. Choi and R. P. Andres, in *Physics and Chemistry of Small Clusters,* edited by P. Jena, B. K. Rao, and S. N. Khanna (Plenum, New York, 1987), p. 61.
[40]E. W. Plummer and T. N. Rhodin, J. Chem. Phys. **49**, 3479 (1968).
[41]S. Giorgio, J. Urgan, and W. Kunath, Philos. Mag. **60A**, 553 (1989).
[42]J. J. Pireaux, M. Chtaib, J. P. Delrue, P. A. Thiry, M. Liehr, and R. Caudano, Surf. Sci. **141**, 211 (1984).
[43]J. Kolaczkiewicz and E. Bauer, Surf. Sci. **175**, 508 (1986).
[44]F. Piuz and J. P. Borel, Phys. Status Solidi A **14**, 129 (1972).
[45]J. R. Sambles, L. M. Skinner, and N. D. Lisgarten, Proc. R. Soc. London A **318**, 507 (1970).
[46]*American Institute of Physics Handbook,* 3rd ed., edited by Dwight E. Gray (McGraw-Hill, New York, 1972).
[47]*CRC Handbook of Chemistry and Physics,* 64th ed., edited by Robert C. Weast (Chemical Rubber, Cleveland, 1983).

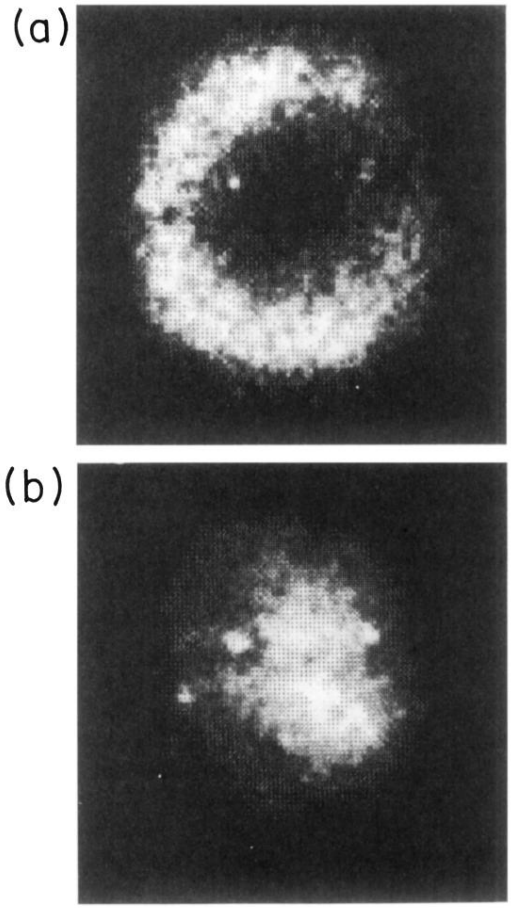

FIG. 4. A digital field-emission pattern of ~80 Å diameter Ag cluster taken after placing the sample into the field-emission chamber. In (a), the pronounced torus-shape geometry is clearly evident. The same sample after heating the substrate to ~400 K is shown in (b). The torus-shape configuration has vanished.